

Low-lying Eigenvalues of the QCD Dirac Operator at Finite Temperature

P.H. DAMGAARD^a, U.M. HELLER^b, R. NICLASSEN^a and K. RUMMUKAINEN^{c,d}

^aThe Niels Bohr Institute and ^cNORDITA
Blegdamsvej 17
DK-2100 Copenhagen, Denmark

^bCSIT
Florida State University
Tallahassee, FL 32306-4130, USA

^dHelsinki Institute of Physics,
P.O.Box 9, 00014 University of Helsinki, Finland

December 2, 2024

Abstract

We compute the low-lying spectrum of the staggered Dirac operator above and below the finite temperature phase transition in both quenched QCD and in dynamical four flavor QCD. In both cases we find, in the high temperature phase, a density with close to square root behavior, $\rho(\lambda) \sim (\lambda - \lambda_0)^{1/2}$. In the quenched simulations we find, in addition, a volume independent tail of small eigenvalues extending down to zero. In the dynamical simulations we also find a tail, decreasing with decreasing mass, at the small end of the spectrum. However, the tail falls off quite quickly and does not seem to extend to zero at these couplings. We find that the distribution of the smallest Dirac operator eigenvalues provides an efficient observable for an accurate determination of the location of the chiral phase transition, as first suggested by Jackson and Verbaarschot.

1 Introduction

The correlations of Dirac operator eigenvalues in QCD and related theories have been shown to have a fascinating relation to Random Matrix Theory. There are two very different domains of interest here. One is the so-called “bulk” of the eigenvalue spectrum of the Dirac operator, far from both the infrared and the ultraviolet ends. The other is the so-called “hard edge” at $\lambda \sim 0$, *i.e.* the infrared end of the spectrum in theories with spontaneous breaking of chiral symmetry. The relevance of Random Matrix Theory in describing eigenvalue correlations of the Dirac operator in the bulk of the spectrum was first demonstrated by Halasz and Verbaarschot [1], and it has since been confirmed by numerous lattice gauge theory studies [2]. From a theoretical point of view, these results in the bulk of the spectrum remain to be better understood. In the other case, near $\lambda \sim 0$, the connection between universal Random Matrix Theory results and the QCD Dirac operator spectrum [3, 4, 5] is by now firmly established, and has also been extensively checked in lattice gauge theory simulations [6]. Already in the original work of Shuryak and Verbaarschot [3] it was shown that the pertinent chiral Random Matrix Theory partition function coincides exactly with the effective field theory partition function in the relevant microscopic limit. More recently an explicit relationship between the universal Random Matrix Theory eigenvalue distributions and those of the QCD Dirac operator has been established [7, 8], the precise link being the partially quenched chiral condensate [8, 9]. In this domain Random Matrix Theory is an intriguing alternative description of exactly the same phenomena that can be derived from the effective QCD partition function in the large-volume limit where $V \ll 1/m_\pi^4$ [10].

There exists also an interesting physical situation that forces us to reconsider the two different domains of the Dirac operator spectrum simultaneously. This is near the finite-temperature chiral phase transition, where the analytical connection between the effective QCD partition function and Random Matrix Theory breaks down even for the part of the spectrum that is close to $\lambda = 0$. This situation is readily confronted in lattice gauge theory. Indeed, it is for staggered fermions even rigorously proven [11], that chiral symmetry is restored at high temperature. The low-lying spectrum of the Dirac operator must therefore be quite different in the high temperature phase as compared with zero temperature. In particular, the absence of chiral symmetry breaking implies, through the Banks-Casher relation,

$$\langle \bar{\psi}\psi \rangle = \pi \rho(0) , \quad (1)$$

that the density of eigenvalues at zero vanishes. This could happen either just at that point of $\lambda = 0$ (as, for example, in the free theory where $\rho(\lambda) \sim \lambda^3$), or the spectrum could develop a gap. The chiral phase transition occurs at the temperature T_c where the density of Dirac operator eigenvalues just reaches zero at $\lambda = 0$. If the transition is continuous, this will happen smoothly as the temperature T is increased towards T_c . In such a case, an important question to settle is the precise power-law behavior of the spectral density of the Dirac operator right at $T = T_c$, because this can be related to the critical exponents of the phase transition [12]. The same chiral Random Matrix Theory that yields universal microscopic spectral correlators which exactly coincide with those of the Dirac operator at $T = 0$ can be tuned in such a way as to just reach (multi-critical) points where [13]

$$\rho(\lambda) \sim \lambda^{2k} \quad (2)$$

near $\lambda = 0$. Here k is an integer labeling the multi-criticality. At such points universality of microscopic spectral correlators still holds in the Random Matrix Theory context, but there is no justification for assuming that these results are relevant for the Dirac operator spectrum at $T = T_c$.¹ There is also a

¹In particular, this behavior is only compatible with a continuous phase transition. But at a more fundamental level, there is simply no longer any relation between the chiral Random Matrix Theory ensemble and the effective QCD partition function for temperatures T that do not satisfy $T \ll \Lambda_{QCD}$.

schematic Random Matrix model for the finite-temperature behavior of the Dirac operator spectrum [14]. It gives a different behavior at $T = T_c$: $\rho(\lambda) \sim \lambda^{1/3}$. Also here there is no physical justification for using it in connection with the Dirac operator spectrum at finite temperature, but it is an interesting model that depends on just one deterministic external parameter, and we shall therefore return to it below.

Suppose, for a moment, that the Dirac spectrum actually develops a gap around $\lambda = 0$ above T_c . In Random Matrix Theory the end of a spectrum around such a gap is referred to as a “soft edge”. Generally, the (macroscopic) density of eigenvalues near a soft edge behaves as (for $\lambda > \lambda_0$) [15]:

$$\rho(\lambda) \propto (\lambda - \lambda_0)^{2m+1/2} \quad (3)$$

with λ_0 being the location of the edge. Here m is an integer that labels universality classes classified by their Random Matrix Theory potentials (m parameters in the potentials must be tuned in order to reach each class). Thus the *generic* behavior, without any fine tuning, corresponds to $m = 0$, which gives a square root approach to the soft edge:

$$\rho(\lambda) \propto (\lambda - \lambda_0)^{1/2} \quad (4)$$

Random Matrix Theory actually gives a more detailed, microscopic, description. This arises from a blowing-up of the eigenvalue density function around the soft edge λ_0 with a rescaling according to the macroscopic behavior (3). For example, for the generic $m = 0$ universality class, the corresponding microscopic eigenvalue density is [16]

$$\rho(\lambda) \propto X[\text{Ai}(-X)]^2 + [\text{Ai}'(-X)]^2, \quad (5)$$

where $X \propto (\lambda - \lambda_0)N^{2/3}$ and $\text{Ai}(x)$ is the standard Airy function. Here N denotes the size of the matrix, and the rescaling by $N^{2/3}$ is required in order to spread out the increasing number of eigenvalues to obtain one well-defined limiting function. From the known asymptotic behavior of the Airy functions one finds:

$$\rho(\lambda) \sim \begin{cases} \frac{\sqrt{X}}{\pi} + \mathcal{O}\left(\frac{1}{X}\right) & \text{for } X \rightarrow \infty \\ \frac{17}{96\pi}|X|^{-1/2} \exp(-4|X|^{3/2}/3) & \text{for } X \rightarrow -\infty \end{cases} \quad (6)$$

Thus, at the microscopic level the spectrum is not cut off sharply at λ_0 , but has an exponentially suppressed tail beyond. Further, the square root behavior of the eigenvalue density is modulated by wiggles corresponding to the distribution of particular eigenvalues (smallest, second, third, etc.). (See, for example, Fig. 9.)

Until a few months ago, there existed only one low-statistics investigation of the low-lying Dirac eigenvalue spectrum for staggered fermions in the high temperature phase [17]. It did not unequivocally establish the existence of a gap. For example, some low eigenvalues were found. However, they could possibly be attributed to “would-be zero modes” from global gauge field topology, shifted away from zero by the explicit chiral symmetry breaking of staggered fermions at finite lattice spacing [18]. This is a general problem with staggered fermions that also we must face here: at finite lattice spacing, the index theorem is not valid for staggered fermions, and gauge field topology (whichever way one defines it on a discrete lattice) does not give rise to exact zero modes of the staggered Dirac operator. At $T = 0$ no trace of non-trivial gauge field topology on the lowest-lying spectrum of staggered eigenvalues has been found [19], except in the 2-d Schwinger model at fairly small lattice spacing [20]. Finite temperature, which causes a depletion of genuine non-zero eigenvalues near $\lambda \sim 0$, further complicates this issue of a mix-up with would-be zero modes.

Very recently a study of just the low-lying Dirac operator eigenvalues near T_c has actually indicated the presence of a gap at large lattice volumes [21]. Again the statistics was rather limited, and only a small number of the lowest-lying eigenvalues could be included (varying between 8 and 10). The present study will in many ways follow the same lines of thought as ref. [21], but we shall have much larger statistics, and we shall also probe some different aspects. In particular, we are also interested in seeing whether quenching causes a different behavior of the smallest eigenvalues near T_c compared with dynamical fermions.

Last year a study of low-lying eigenvalues of the overlap Dirac operator in quenched finite temperature gauge theories appeared [22]. Overlap fermions are well suited for such an investigation since they do not suffer from explicit chiral symmetry breaking even at finite lattice spacing and since they have exact zero modes in topologically non-trivial gauge fields. Ref. [22] found that effects of topology persisted in the high temperature phase, although strongly suppressed compared to the low temperature phase. More interestingly, an accumulation of low eigenvalues with an apparently finite density in the infinite-volume limit was found very near $\lambda \sim 0$ even above the (quenched) phase transition temperature T_c . The statistical properties of the smallest group of eigenvalues were consistent with them being due to a dilute gas of instantons and anti-instantons [22]. These results have led to the speculation that chiral symmetry might remain broken even in the high temperature phase of quenched QCD with overlap fermions.

In this paper we describe high statistics investigations of the low-lying eigenvalue spectrum of the staggered Dirac operator for SU(3) gauge group at finite temperature. We do this for both quenched (section 2) and dynamical QCD with four flavors of staggered fermions (section 3). The interest in the quenched case lies primarily in checking whether also staggered fermions, although insensitive to topology at the gauge couplings we can investigate here, show signs of unusual behavior of the smallest Dirac eigenvalues above T_c (as was the case for overlap fermions [22]). Both quenched and unquenched simulations give rise to Dirac operator spectra that can be compared with Random Matrix Theory. In particular, if the Dirac operator spectrum exhibits a gap, is it of the soft-edge kind of Random Matrix Theory? Are there indications that Random Matrix Theory provides a more accurate description of the Dirac operator spectrum as the three-volume is increased? We shall try to answer these questions in what follows.

2 Quenched QCD at high temperature

For our quenched finite temperature Monte Carlo simulations we have used lattices with temporal extent $N_t = 4$ and up to three spatial volumes: 8^3 , 12^3 and 16^3 . For $N_t = 4$ the deconfinement phase transition for SU(3) pure gauge theory with Wilson action has been very accurately determined, occurring at lattice gauge coupling $\beta_c = 5.6925(2)$ [23]. It has for long been assumed that the chiral phase transition of the quenched theory occurs at exactly this deconfinement phase transition point of the pure gauge theory, but this has recently been challenged [22].

We now give some technical details of our simulations. The gauge field configurations were generated with a mixture of overrelaxation and heat bath updates, and were analyzed after every 20-th heat bath sweep. On each configuration we computed the 50 lowest-lying eigenvalues, and in some cases even more, using the variational Ritz functional method [24]. Many ensembles consisted of several thousand configurations. Gauge coupling, lattice size and statistics of our ensembles is summarized in Table 1.

V	β	#configurations
$8^3 \times 4$	5.5	5931
$8^3 \times 4$	5.66	5544
$8^3 \times 4$	5.695	1769
$8^3 \times 4$	5.71	1145
$8^3 \times 4$	5.72	1426
$8^3 \times 4$	5.73	2021
$8^3 \times 4$	5.75	7029
$12^3 \times 4$	5.75	1933
$16^3 \times 4$	5.75	692
$8^3 \times 4$	5.8	5335
$8^3 \times 4$	5.85	6149
$8^3 \times 4$	5.9	4263
$12^3 \times 4$	5.9	1755
$16^3 \times 4$	5.9	824

Table 1: Details of our quenched ensembles.

As is well-known, the staggered Dirac operator

$$\begin{aligned}
D_{x,y} &= \frac{1}{2} \sum_{\mu} \eta_{\mu}(x) \left(U_{\mu}(x) \delta_{x+\mu,y} - U_{\mu}^{\dagger}(y) \delta_{x,y+\mu} \right) \\
&\equiv D_{e,o} + D_{o,e}
\end{aligned} \tag{7}$$

is anti-hermitian, with purely imaginary eigenvalues $i\lambda$ that come in pairs of opposite sign. In eq. (7)

$$\eta_{\mu}(x) = (-1)^{\sum_{\nu < \mu} x_{\nu}} \tag{8}$$

are the usual phase factors for staggered fermions. Denoting

$$\epsilon(x) = (-1)^{\sum_{\nu} x_{\nu}}, \tag{9}$$

we have also explicitly shown how D connects *even* sites, i.e. those with $\epsilon(x) = +1$, with *odd* sites, those with $\epsilon(x) = -1$, and vice versa. This means that the operator $-D^2$ is hermitian and positive semi-definite. The sign function $\epsilon(x)$ defined above plays the role of γ_5 in the continuum: it anticommutes with D : $\{D, \epsilon\} = 0$. As $-D^2$ does not mix between even and odd lattice sites, we need only compute the eigenvalues, on, say, the even sublattice. One easily sees that if ψ_e is a normalized eigenvector of $-D^2$ with eigenvalue λ^2 , then $\psi_o \equiv \frac{1}{\lambda} D_{o,e} \psi_e$ is a normalized eigenvector of $-D^2$ with eigenvalue λ^2 , and non-zero only on odd sites. Moreover, as we will never encounter exact zero modes on genuine quantum configurations, there is no difficulty with the above definition of ψ_o . We of course make use of these properties, and hence compute only the (positive) eigenvalues of $-D^2$ restricted to the even sublattice, and then take the (positive) square root. All eigenvalues to be shown in the following thus have an equal number of negative companions, of the exact same magnitude.

The spectral density of the Dirac operator is given by

$$\rho(\lambda) \equiv \frac{1}{V} \langle \sum_n \delta(\lambda - \lambda_n) \rangle, \tag{10}$$

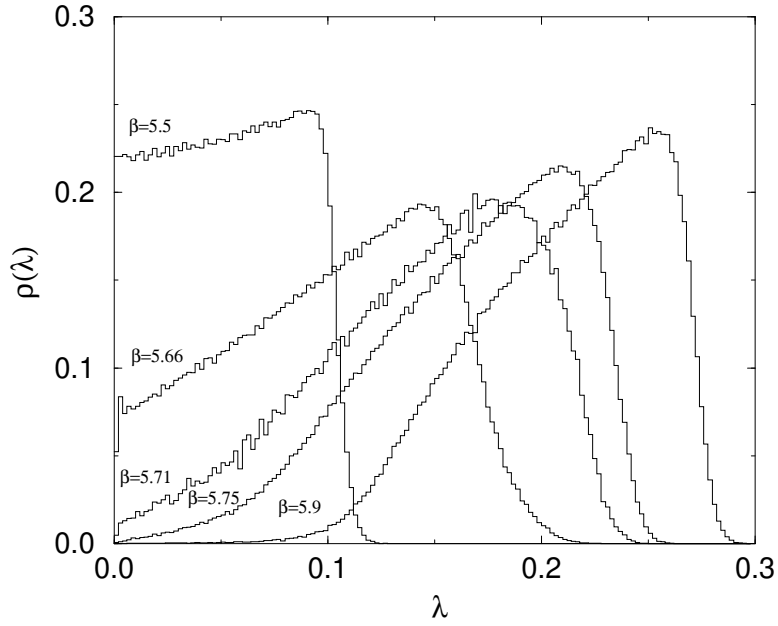


Figure 1: The measured distribution of the 50 lowest eigenvalues in quenched QCD at finite temperature for several β 's on $8^3 \times 4$ lattices. One sees a clear suppression of the spectral density at the origin $\rho(0)$ as the temperature (coupling) is increased, indicating a diminishing chiral condensate according to the Banks-Casher formula. For large temperatures the spectrum is heavily suppressed near the origin, although in this quenched case a small tail always seems to extend towards $\lambda = 0$ (see below).

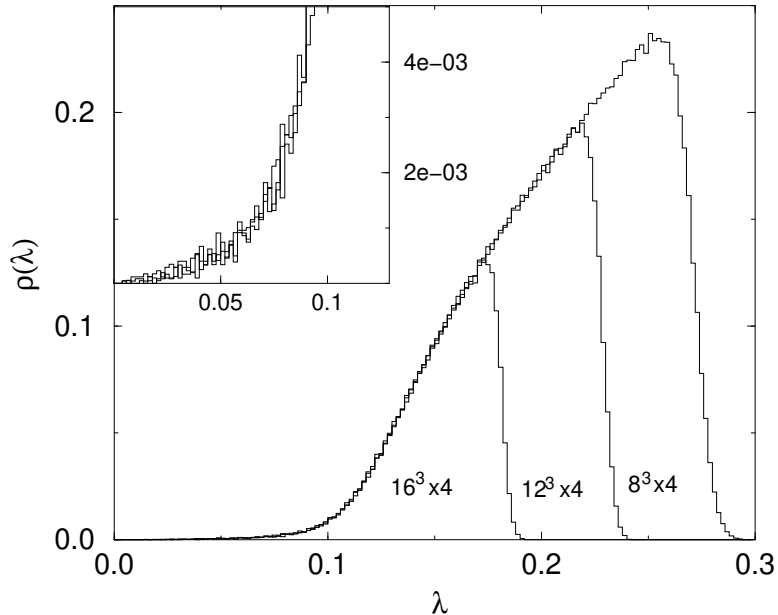


Figure 2: The density of the smallest eigenvalues in the high temperature phase of quenched QCD, at $\beta = 5.9$, for spatial volumes 8^3 , 12^3 and 16^3 . In the two large volumes we measured 100 eigenvalues and only 50 in the small volume. Since the eigenvalue density increases with increasing volume, the distributions are correspondingly cut off at smaller λ . There is no observable change in the eigenvalue density as the three-volume is increased. This holds even at the very small tail extending towards $\lambda = 0$, as shown in the magnified plot inserted.

and it is readily computed numerically from our Monte Carlo simulations by a binning of the measured eigenvalues per configuration at convenient small intervals.

In Fig. 1 we show the density of low lying eigenvalues on $8^3 \times 4$ lattices for several β values between 5.5 (in the confined phase) to 5.9 (in the deconfined phase). In each case we computed the 50 lowest positive eigenvalues $i\lambda$ of the staggered Dirac operator. The plots are normalized by the following condition, $\int_0^\infty \rho(\lambda) d\lambda = \#\text{eigenvalues}/V$. In the confined phase it is quite evident that the density at zero would be non-zero in the thermodynamic limit. As the temperature is increased, the density at zero decreases. There is a qualitative change of the eigenvalue density once the temperature is increased above T_c . Beyond the first few eigenvalues the eigenvalue density assumes a shape compatible with a square root behavior (4). However, a sizable tail, decreasing with increasing temperature, of small eigenvalues persists, which seems to extend all the way down to zero.

In Fig. 2 we compare the eigenvalue density in the high temperature phase, at $\beta = 5.9$, for several spatial volumes. As can be seen the eigenvalue density is volume independent to a surprising degree. In particular, the tail of small eigenvalues is seen to be volume independent and appears to persist in the thermodynamic limit. We note that the tail is much larger than would be compatible with the exponential tail from the Airy function behavior of random matrix theory at a soft edge eq. (6) (see Fig. 9 in section 3 below for an example).

It is tempting to speculate that the tail seen here in the quenched case with staggered fermions is a

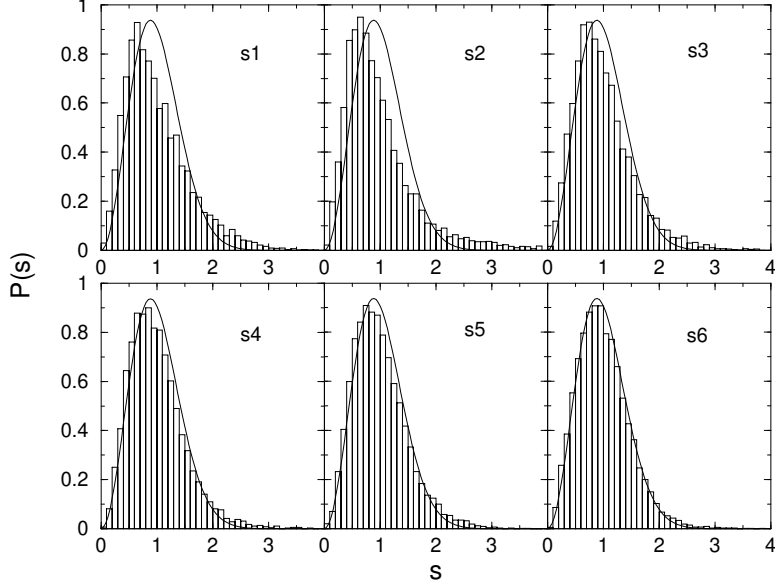


Figure 3: Distributions of the unfolded level spacings between the first few eigenvalues for $\beta = 5.75$ on an $8^3 \times 4$ lattice, compared to the Wigner surmise. The agreement with Random Matrix Theory is clear once we go beyond the first few eigenvalues. However, there is not very good agreement for the first 2-3 eigenvalues at this volume.

reflection of the accumulation of small eigenvalues seen with overlap fermions in [22] and attributed there to a dilute gas of instantons and anti-instantons. In the staggered case, the explicit chiral symmetry breaking at finite lattice spacing shifts the small modes, presumably resulting in the observed tail.

We also looked at the unfolded level spacing between individual eigenvalues i and $i + 1$

$$s_i = \frac{\lambda_{i+1} - \lambda_i}{\langle \lambda_{i+1} - \lambda_i \rangle}. \quad (11)$$

In Fig. 3 the distribution of the s_i between eigenvalue i and $i + 1$, $i = 1..6$ is shown and compared to the expected distribution, the Wigner surmise

$$P(s) = \frac{32}{\pi^2} s^2 e^{-\frac{4}{\pi} s^2}. \quad (12)$$

Evidently, the level spacings between the first eigenvalues are not very accurately given by Random Matrix Theory correlations. But as we move into the bulk, say for $i > 5$ in the case of the $8^3 \times 4$ lattice, the agreement with Random Matrix Theory becomes almost perfect. It should be stressed here that this is a volume-dependent statement. For larger volumes one needs to go beyond more eigenvalues starting at the soft edge before one finds good agreement. This is consistent with the fact that there is a definite scale around the soft edge, where eigenvalue correlations are poorly described by Random Matrix Theory. Going to larger volumes simply forces more eigenvalues into that region.

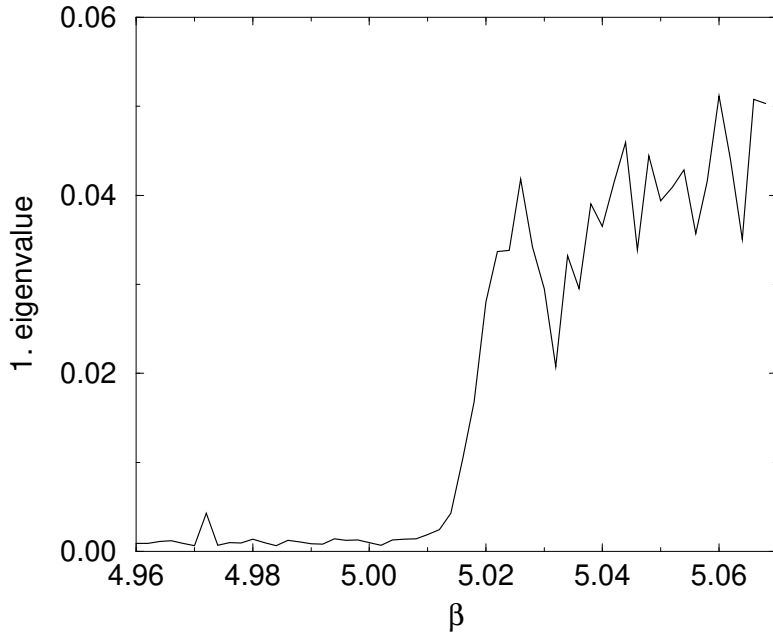


Figure 4: The lowest eigenvalue, averaged over 5 configurations, on an $8^3 \times 4$ lattice with $am_q = 0.025$ as a function of β . One sees a clear change in behavior around $\beta \sim 5.02$, indicating the restoration of chiral symmetry around this temperature. Just this first Dirac operator eigenvalue can thus serve as an excellent indicator of the chiral phase transition point.

3 QCD with four dynamical fermions at high temperature

For our dynamical simulations we chose to work with $n_f = 4$ flavors. Four is the “natural” number of flavors for staggered fermions in the continuum limit, and an efficient exact simulation algorithm can be used, the Hybrid Monte Carlo algorithm. In addition, the four flavor theory is known to have a rather strong first order finite temperature phase transition [25]. Therefore, tunnelings into the low temperature phase are strongly suppressed already on rather small systems and at temperatures quite close to T_c .

We made dynamical simulations with quark masses $am_q = 0.1, 0.05, 0.025, 0.01$ and 0.002 , and for couplings β in the high temperature phase (here a is the lattice spacing). Interestingly, the lowest eigenvalue provides a sensitive method for determining the critical coupling $\beta_c(am_q)$: in Fig 4 the lowest eigenvalue on a $8^3 \times 4$ lattice with $am_q = 0.025$ is plotted against β . β ranges from 4.96 to 5.07 in intervals of 0.002. Each point is an average over 5 configurations at that β -value. A rise is observed between $\beta = 5.012$ and $\beta = 5.022$, which can be clearly interpreted as the chiral symmetry restoring finite temperature phase transition. (For published values of the critical couplings $\beta_c(am_q)$) see ref. [25].) The possibility of using the magnitude of the smallest Dirac operator eigenvalues as probes for chiral symmetry restoration was suggested by Jackson and Verbaarschot [14] on the basis of a similarly observed behavior in a Random Matrix Theory context that we will also discuss below.

Most of our analysis with dynamical fermions was performed at $\beta = 5.2$, which is above β_c for all values of m_q we used. Typically, we analyzed ~ 3000 configurations for each volume and m_q , extracting the 50 smallest eigenvalues. Ensemble details are summarized in Table 2. Note the large statistics

V	β	am_q	#configurations
$8^3 \times 4$	5.1	0.1	8897
$8^3 \times 4$	5.1	0.025	2909
$8^3 \times 4$	5.1	0.01	4050
$8^3 \times 4$	5.2	0.1	4348
$8^3 \times 4$	5.2	0.05	2149
$8^3 \times 4$	5.2	0.025	29632
$12^3 \times 4$	5.2	0.025	13929
$8^3 \times 4$	5.2	0.01	4050
$12^3 \times 4$	5.2	0.01	2882
$8^3 \times 4$	5.2	0.008	4200
$8^3 \times 4$	5.2	0.005	7948
$8^3 \times 4$	5.2	0.002	6950
$8^3 \times 4$	5.3	0.025	4549
$8^3 \times 4$	5.4	0.025	3746

Table 2: Details of our ensembles with dynamical fermions.

gathered for $\beta = 5.2$ and $am_q = 0.025$.

As in the quenched case we find a small tail at the lower end of the eigenvalue distribution, reaching towards $\lambda = 0$ from the main bulk of the distribution. This tail also appears to be volume independent (see Fig. 6). However, in this case it is somewhat more suppressed than in the quenched case, and for small values of the quark mass it does not extend all the way to $\lambda = 0$, see Fig. 5.

In Fig. 7 we show eigenvalue distributions measured at $\beta = 5.2$ and various am_q . Note that for larger am_q , β_c is also larger, which causes a shift of the whole spectrum as am_q is varied. Therefore, a direct quantitative comparison of the distributions in Fig. 7 is not straightforward. However, we note that the distributions at $am_q = 0.025$ and $am_q = 0.002$ are almost on top of each other, indicating that these distributions are very close to the $am_q = 0$ distribution.

Furthermore, as in the quenched case described in the previous section, we find the “macroscopic” behavior of the eigenvalue density seemingly compatible with a square root form. By fitting eq. (3) to the bulk of the spectrum (leaving out the tail), we obtain different powers, depending on how much of the tail we choose to cut off. This fitting has been done for $V = 8^3 \times 4$ at $\beta = 5.2$ and $am_q = 0.025$ and the resulting values can be seen in Table 3. There is a clear tendency towards a slightly higher power ($= 2m + 1/2$) than the square root which would be expected from Random Matrix Theory. In Fig. 8 we show the fit with the cut at 0.1. For comparison, we include the distribution of the first eigenvalue in the figure. Clearly, the tail at small λ is caused by the excessive width of the distribution of the smallest eigenvalue.

In Fig. 9 we compare the spectral density for quark mass $am_q = 0.025$ with the prediction (5) of the Random Matrix Theory for the density near a soft edge. In order to make the comparison possible, we rescale the spectral density as

$$\rho(\lambda) \rightarrow \frac{\lambda_0}{2} \left(\frac{2}{\pi \lambda_0 K V} \right)^{\frac{2}{3}} \rho \left(\frac{2}{\lambda_0} (\lambda - \lambda_0) \left(\frac{2}{\pi \lambda_0 K V} \right)^{-\frac{2}{3}} \right) \quad (13)$$

where we determine λ_0 and K from a fit to a square root: $\sqrt{\frac{\lambda_0}{2}} K \sqrt{(\lambda - \lambda_0)}$. Here V is the lattice vol-

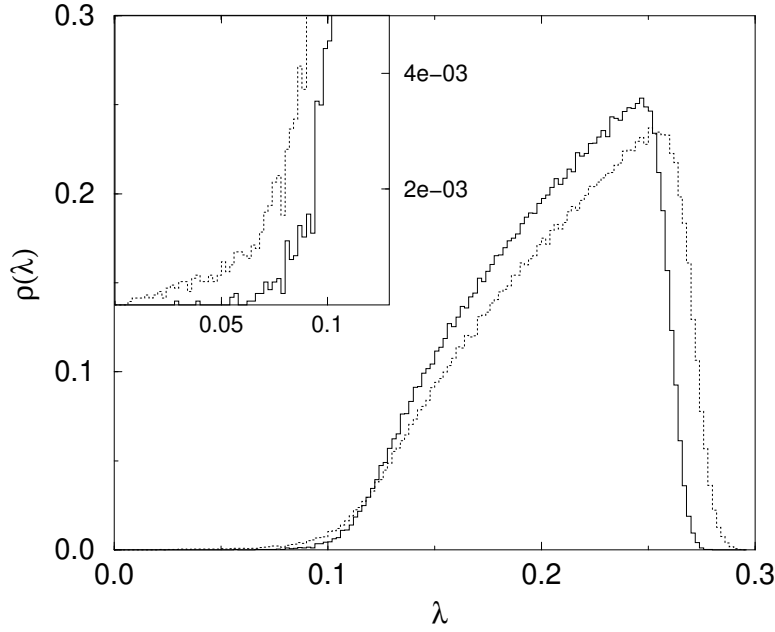


Figure 5: Quenched spectrum of $\beta = 5.9$ and a dynamical spectrum at $\beta = 5.4$ with $am_q = 0.025$, both on an $8^3 \times 4$ lattice. A blowup of the y-axis near the end of the tail is also shown. There is a much stronger suppression of small eigenvalues in the case of dynamical fermions, perhaps due to fewer would-be zero modes in topological non-trivial gauge field configurations.

Cut at	m	$2m + 1/2$
0.09	0.055 ± 0.003	0.609 ± 0.006
0.095	0.049 ± 0.004	0.598 ± 0.007
0.1	0.040 ± 0.005	0.580 ± 0.010
0.105	0.036 ± 0.006	0.572 ± 0.011
0.11	0.041 ± 0.008	0.582 ± 0.016
0.115	0.035 ± 0.010	0.570 ± 0.019
0.12	0.043 ± 0.013	0.585 ± 0.027
0.125	0.040 ± 0.016	0.581 ± 0.032
0.13	0.033 ± 0.021	0.567 ± 0.041
0.14	0.027 ± 0.034	0.554 ± 0.068

Table 3: The dependence of the fitted power on the λ where the small- λ tail is cut off. The data are from $8^3 \times 4$, $\beta = 5.2$ and $am_q = 0.025$ lattices, using the 50 smallest eigenvalues. The fits are almost compatible with a square-root behavior of the spectrum at this soft edge, but there is a consistent small upward shift in the exponent.

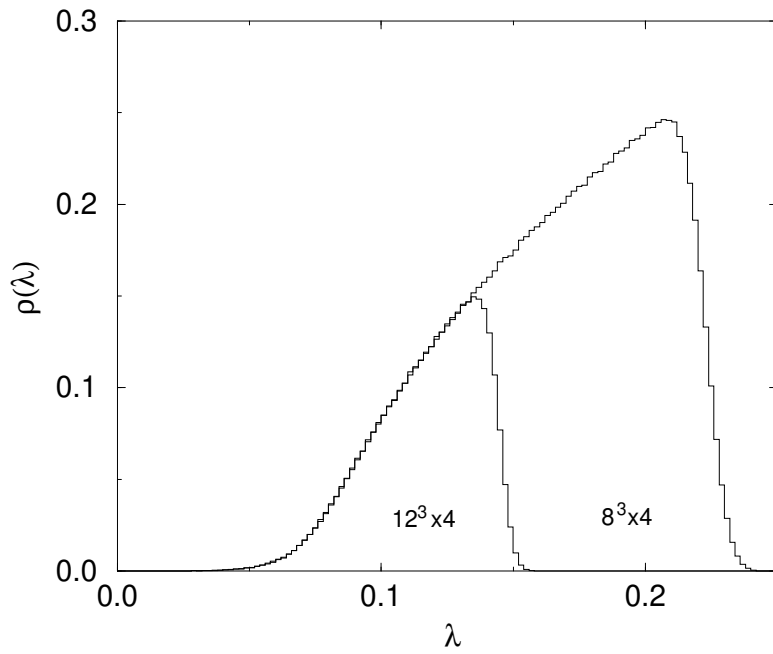


Figure 6: The density of the 50 smallest eigenvalues in the high temperature phase, $\beta = 5.2$ and $am_q = 0.025$ for spatial volumes 8^3 and 12^3 . The normalization of the distributions is as in Fig. 2. As in the quenched simulations, we observe no significant change in the eigenvalue spectrum at all as the three-volume is increased.

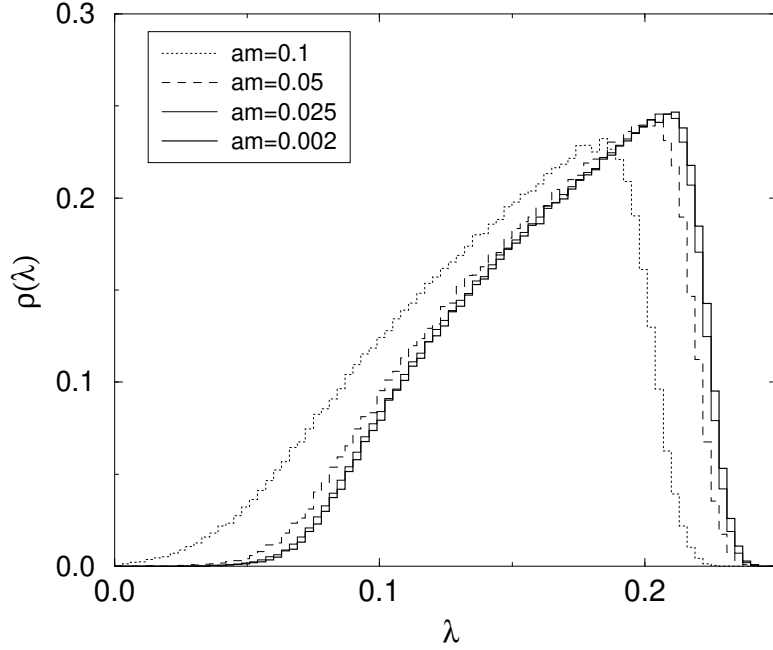


Figure 7: The density of the 50 smallest eigenvalues at $\beta = 5.2$ for quark masses $am_q = 0.1, 0.05, 0.025, 0.002$ on $8^3 \times 4$ lattices. While there is some shift with decreasing quark mass for the larger values of am_q , the spectral density seems to approach a limiting function, which we can identify as the chiral limit of the spectrum. Note that the large-mass behavior of the spectrum is almost identical to the quenched spectrum in this region, in agreement with the notion that on this scale of eigenvalues the large-mass fermion has completely decoupled, and effectively become quenched.

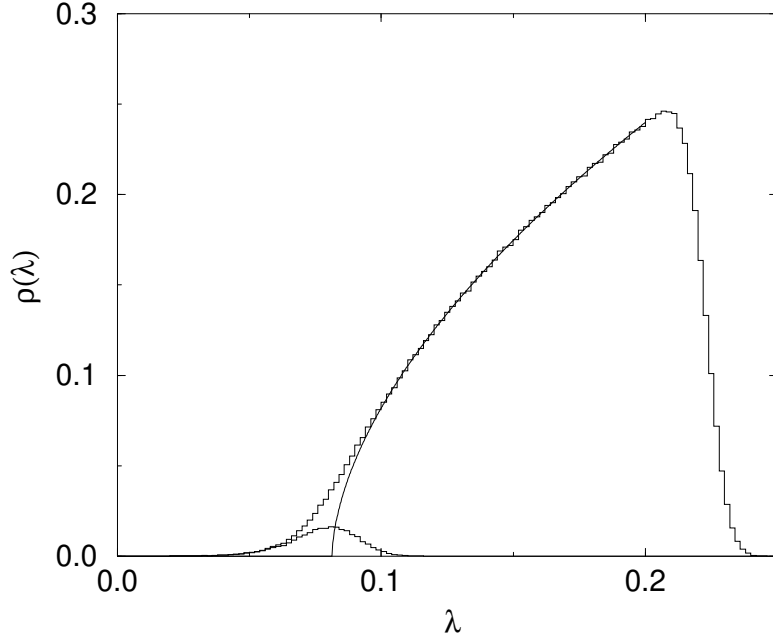


Figure 8: Power fit to the spectral density for $\beta = 5.2$ with $am_q = 0.025$ on an $8^3 \times 4$ lattice with cut at 0.1 (see Table 3). Also included is the distribution of the first eigenvalue. The distribution of this smallest eigenvalue is very different from that demanded by the Airy-function behavior (see below).

ume. We see that the tail predicted by the Random Matrix Theory is much more strongly suppressed than the measured distribution. Moreover, we can also observe that the density of the eigenvalues themselves does not match: the measured distribution includes 50 eigenvalues, whereas the function (5) has only 40 ‘wiggles’ in the λ -range of the distribution. However, if we attempt to perform the comparison by matching the number of eigenvalues/wiggles, the overall fit becomes worse. In itself, this mismatch is not surprising, when we remember that the overall shape is *not* well described by a square root behavior in the first place (see Table 3).

In the quenched simulations we saw that correlations between the first 5 or 6 eigenvalues were not very accurately given by Random Matrix Theory. In Fig. 10 the distribution of s_i , defined in eq. (11), is shown for a dynamical simulation with $\beta = 5.2$, $am_q = 0.025$ on a $8^3 \times 4$ lattice. Here we see, on the same lattice volume, a clear deviation from the Wigner surmise only for the first two or three spacings, s_1 , s_2 and s_3 . Again, comparisons can only be made at equal volumes, as larger volumes imply more eigenvalues in the region around the soft edge where correlations are poorly described by Random Matrix Theory.

There is an interesting physical consequence of a genuine gap in the Dirac eigenvalue spectrum. Consider the difference between the (π) susceptibility χ_P and the susceptibility of its scalar partner (a_0), which we denote by χ_S [26, 27]. In a manner similar to the Banks-Casher formula for the chiral condensate one finds that this difference can be written

$$\omega = 4m^2 \int_0^\infty d\lambda \frac{\rho(\lambda; m)}{(\lambda^2 + m^2)^2}, \quad (14)$$

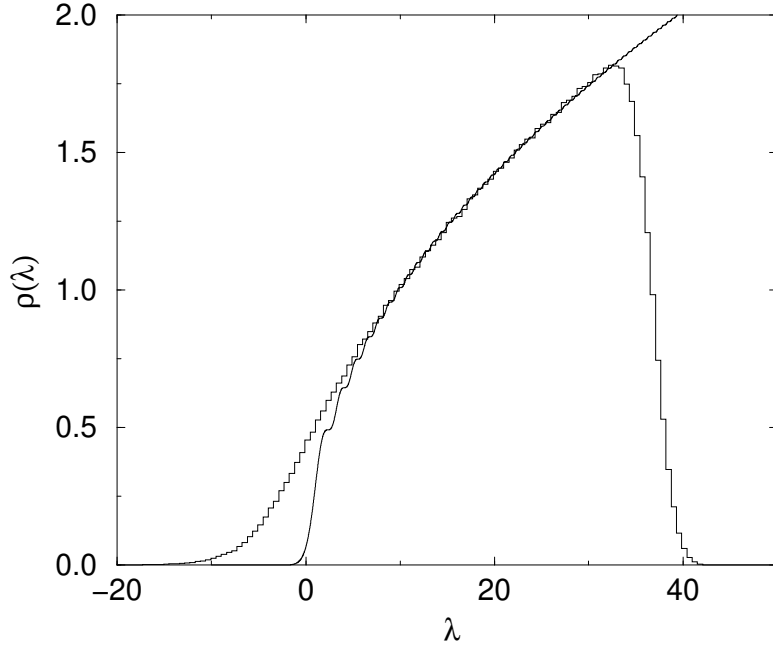


Figure 9: Comparison of the spectral density for $\beta = 5.2$, $am_q = 0.025$ on a $8^3 \times 4$ lattice, with the Random Matrix Theory prediction for a soft edge, as in eq. (5).

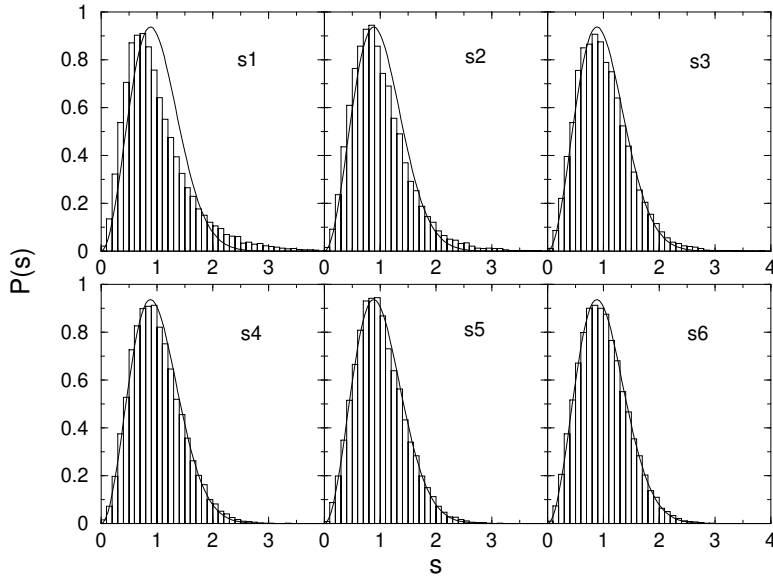


Figure 10: Distributions of the unfolded level spacings between the first few eigenvalues in the dynamical case, compared to the Wigner surmise. As in the quenched case, we find a small disagreement for the first eigenvalues. But in contrast to the quenched case the agreement sets in after almost just the 2nd eigenvalue, at the same volume.

where the spectral density $\rho(\lambda; m)$ includes the zero modes due to topology as well. In the infinite-volume limit this contribution from exact zero modes should vanish, and we should be left with the integral over non-zero modes. If the spectral density has a gap around the origin this means that ω vanishes in the chiral limit. Because axial U(1) rotates χ_P into χ_S and vice versa, this would imply a restoration of axial U(1) at these high temperatures [26, 27]. Conversely, if one believes that this axial U(1) symmetry is *not* restored at high temperature, one gets constraints on the behavior of the spectral density of the Dirac operator near the origin. For a power-law behavior near $\lambda \sim 0$ a non-vanishing ω in the infinite-volume chiral limit can only be supported for $\rho(\lambda, 0) \sim \lambda^\alpha$ with $\alpha \leq 1$, and in fact ω would only remain finite in that limit if $\alpha = 1$.

Of course, the fact that we appear to see a gap in the eigenvalue spectrum with staggered fermions at this particular coupling does not imply that this gap persists in physical units as we take the continuum limit. If not, we are here studying a pure lattice artifact. The only way to test this is to study the shift in the apparent cut-off eigenvalue λ_0 as we change the lattice spacing (this is, however, far beyond what we can do at present). A very different uncertainty comes from the fact that we are working with fermions that are almost insensitive to topology at the couplings and volumes available to us. This means that there are some would-be zero modes mixed up with our regular eigenvalues near the origin. At zero temperature we found that these would-be zero modes somewhat surprisingly behaved as the non-zero eigenvalues at realistic couplings and volumes [19]. But there is no guarantee that this is the case at finite temperature. This means that the small tail extending to zero in our quenched simulations, and some of the smallest eigenvalues in the simulations with dynamical fermions may be due to these would-be zero modes. In particular, the disagreement with Airy-function behavior very close to the soft edge may be partly due to these would-be zero modes.

4 Random Matrix Theory

We have just shown our lattice gauge theory data for the spectrum of the Dirac operator below, around, and above T_c , and compared it with some of the analytical formulas of Random Matrix Theory in the limit where the size of these matrices N goes to infinity. It is of interest to see how a simple *model* of a chiral phase transition in Random Matrix Theory behaves at finite N , as some external parameter (mimicking temperature T) is changed. The model we shall focus on here was proposed by Jackson and Verbaarschot in the first of ref. [14]. It is based on a modified chiral ensemble of $N \times N$ complex matrices W , with partition function

$$\mathcal{Z} = \int dW \prod_{f=1}^{N_f} \det(M - im_f) \exp \left[-N \text{Tr}(WW^\dagger) \right] \quad (15)$$

in a sector of topological charge zero. Here

$$M = \begin{pmatrix} 0 & W^\dagger + T \\ W + T & 0 \end{pmatrix} \quad (16)$$

is a $2N \times 2N$ block hermitian matrix, and the external deterministic parameter T is playing a rôle reminiscent of temperature. In the normalization chosen here, a continuous “phase transition” occurs at $T_c = 1$, where the spectral density $\rho(\lambda)$ of the eigenvalues of the random matrices just reaches zero [14]. For $T > T_c$ the spectrum becomes two-banded, with a gap surrounding zero. The global shape of $\rho(\lambda)$ in this model will be very different from the actual (macroscopic) Dirac operator spectral density. But the interesting feature lies in having here a simple model which qualitatively seems to describe

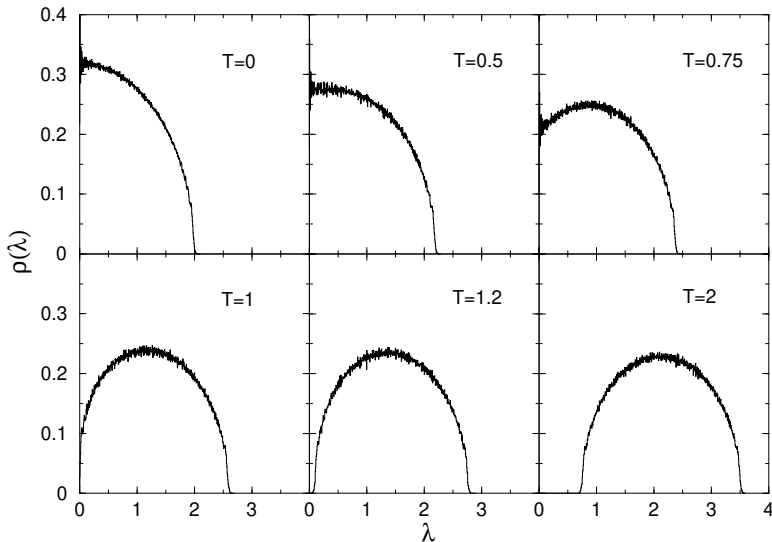


Figure 11: Full spectra of 200×200 matrices at $T = 0, 0.5, 0.75, 1.0, 1.2, 2.0$. In this simple model a gap indeed develops around $\lambda = 0$ at $T = 1$.

some of the observed behavior of the staggered Dirac operator with $N_f = 4$, in particular the apparent gap in the density for $T > T_c$.²

It is very simple to do quenched (*i.e.*, $N_f = 0$) numerical simulations of the above Random Matrix model, as it just corresponds to generating an ensemble of complex matrices with Gaussian weight. Such matrices are “maximally random” in that their matrix elements are independently of Gaussian distribution. This allows us to choose very large random matrices numerically, and then finding the eigenvalues of the hermitian matrix M . In this way we have studied the detailed behavior of the finite- N Random Matrix model (15) just below T_c , at T_c , and just above T_c (where the two bands separate as the gap develops).³

We show some of our numerical results in Figs. 11 and 12. First, in Fig. 11 we display a sequence of the macroscopic spectral density with increasing magnitude of the parameter T : $T = 0, 0.5, 0.75, 1.0, 1.2, 2.0$. The plots were made by diagonalizing 10000 200×200 matrices. At $T = 0$ this macroscopic Random Matrix Theory spectrum is just the Wigner semi-circle law (we display only the $\lambda > 0$ part):

$$\rho(\lambda, T = 0) = \frac{1}{2\pi} \sqrt{4 - \lambda^2} . \quad (17)$$

As T increases, a dip in the spectral density around $\lambda = 0$ slowly develops, and it subsequently turns into a gap. Of course, this macroscopic Random Matrix Theory spectrum is totally unlike the macroscopic Dirac operator spectrum. But it is interesting to zoom in on the microscopic behavior

²Many other details do not match at all. For instance the “phase transition” in the model (15) is continuous, in contrast to the finite-temperature phase transition in the massless $N_f = 4$ theory, which is believed to be of first order.

³Similar numerical studies have been performed by K. Splittorff, M.Sc. thesis, The Niels Bohr Institute 1999 (unpublished). Simulations of the macroscopic spectral density in this model can also be found in the original paper by Jackson and Verbaarschot [14].

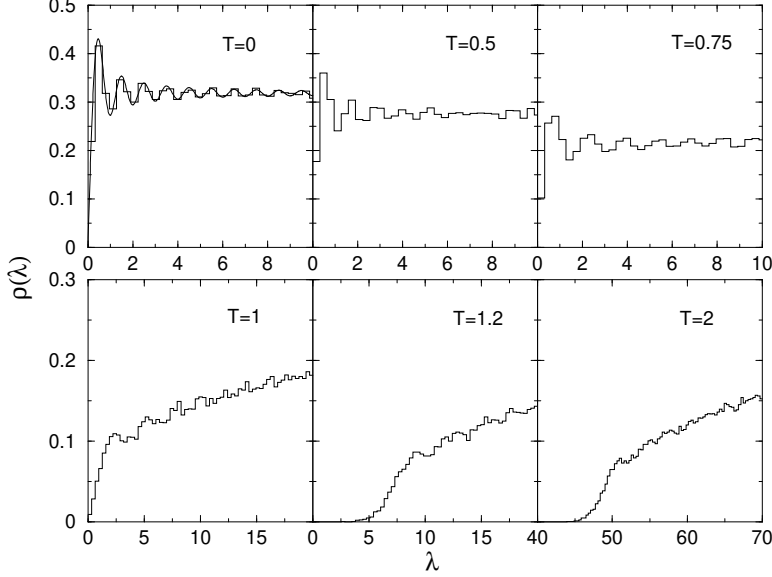


Figure 12: A blowup of the graphs in Fig. 11. The microscopic spectrum changes smoothly from Bessel-type behavior to Airy-type behavior, going through an intermediate “critical” distribution at $T = 1$ corresponding to a macroscopic power-law behavior of type $\rho(\lambda) \sim \lambda^{1/3}$.

of the Random Matrix spectral density at the soft edge of the gap. In this way, by blowing up the scale of the smallest eigenvalues, we obtain the plots in Fig. 12 for the same parameter values of T as above. One sees clearly how the universal Bessel-kernel behavior below T_c turns into the also universal Airy-kernel above T_c . We note that it has been shown in ref. [14] that the massless microscopic spectral density of the above Random Matrix model has precisely the usual zero-temperature form,

$$\rho_s(\zeta(T)) = \frac{\zeta(T)}{2} \left[J_{N_f}(\zeta(T))^2 - J_{N_f-1}(\zeta(T))J_{N_f+1}(\zeta(T)) \right], \quad (18)$$

where $\zeta(T)$ is simply the eigenvalues rescaled by the (T -dependent) infinite-volume spectral density at the origin $\rho(0, T)$:

$$\zeta(T) = \lambda 2\pi N \rho(0, T). \quad (19)$$

In this model $\rho(0)$ approaches zero with a mean-field type of behavior [14]:

$$\rho(0, T) = \rho(0, 0) \sqrt{1 - T^2}. \quad (20)$$

For T bigger than T_c , but still close to it, we find, as expected, a deformation of the Airy-kernel. In fact, the microscopic behavior there smoothly interpolates between the Bessel-form and the Airy-form. The peaks corresponding to individual eigenvalues from the Bessel-function behavior below T_c gradually smoothen out to become the inflection points in the spectral density of the Airy-kind as the soft edge moves away from the origin. To illustrate how accurately one reproduces the Airy-behavior in this kind of simulations, we show in Fig. 13 the soft edge prediction appropriately scaled to fit simulation data at $T=3$. The Airy-behavior is perfectly reproduced close to the edge, but with deviations after the first few eigenvalues(wiggles). The deviation is presumably caused by the limited number of eigenvalues at $N = 300$, and when N is increased we expect the fit to improve.

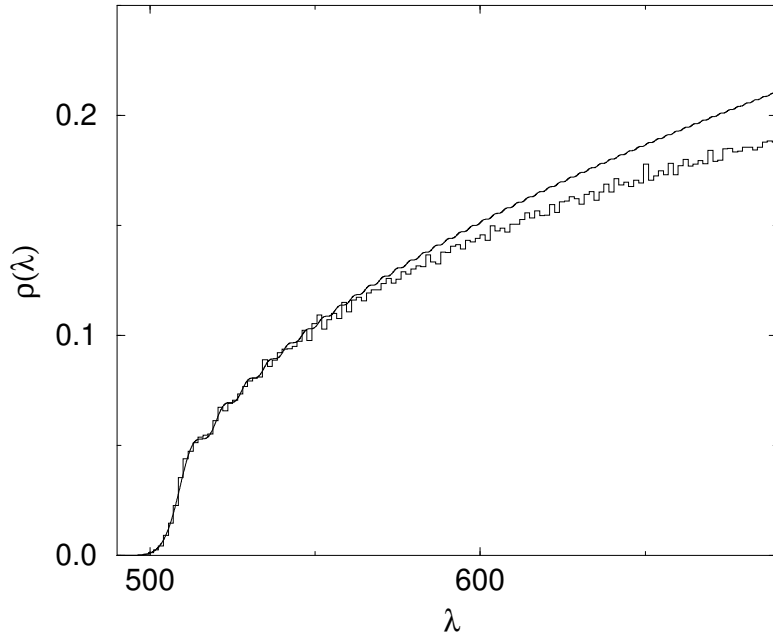


Figure 13: A blowup of a $T = 3$ spectrum compared with the Airy-prediction. There is nice agreement near the edge.

5 Conclusions

The purpose of this study has been to find the extent to which Random Matrix Theory may be able to describe low-lying eigenvalue distributions and correlations between low-lying eigenvalues of the staggered Dirac operator at finite temperature. We have also been interested in testing the quenched theory with staggered fermions in the light of recent results with overlap fermions [22], which indicated that the chiral finite-temperature phase transition in the quenched theory may be more subtle than previously expected. In the quenched case we do not see the accumulation of small Dirac operator eigenvalues around $\lambda = 0$ that was observed with overlap fermions. This is not entirely surprising in view of the insensitivity of staggered fermions to gauge field topology at these lattice couplings and lattice volumes [19, 20]. With staggered fermions we do observe a strong depletion of eigenvalues near the origin once the temperature T reaches the pure gauge theory deconfinement phase transition temperature T_c . This is in agreement with the conventional picture that chiral symmetry is restored in the quenched theory with staggered fermions at precisely the deconfinement phase transition.

On the other hand, we find a clear difference in the behavior of the smallest Dirac operator eigenvalues in the quenched theory and the theory with genuine, dynamical, fermions. In the quenched case a small, volume independent tail of the eigenvalue distribution extends to $\lambda = 0$ while in the full theory the tail does not reach the origin at the couplings we have investigated. While the bulk of the eigenvalue distribution near the (soft) edge is roughly compatible with a square root behavior, the tail of small eigenvalues is considerably larger than the Airy function behavior that Random Matrix Theory would predict. Physically, a genuine gap in physical units in the eigenvalue spectrum above T_c would imply the restoration of axial $U(1)$ symmetry at these high temperatures. A very likely scenario is therefore that the apparent gap found with staggered fermions at finite bare coupling β shrinks to

zero in physical units as the continuum limit is reached. However, an investigation of whether this is indeed the case is much beyond the scope of the present paper.

ACKNOWLEDGMENTS: We thank K. Splittorff and J. Verbaarschot for discussions. The work of P.H.D. and K.R. has been partially supported by EU TMR grant no. ERBFMRXCT97-0122, and the work of U.M.H. has been supported in part by DOE contracts DE-FG05-85ER250000 and DE-FG05-96ER40979. In addition, P.H.D. and U.M.H. acknowledge the financial support of NATO Science Collaborative Research Grant no. CRG 971487.

References

- [1] M.A. Halasz and J.J.M. Verbaarschot, Phys. Rev. Lett. **74** (1995) 3920
- [2] R. Pullirsch, K. Rabitsch, T. Wettig and H. Markum, Phys. Lett. **B427** (1998) 119.
M.E. Berbenni-Bitsch *et al.*, Phys. Lett. **B438** (1998) 14.
J. Ma, T. Guhr and T. Wettig, Eur. Phys. J. **A2** (1998) 87.
T. Guhr, J.Z. Ma, S. Meyer and T. Wilke, Phys. Rev. **D59** (1999) 054501.
B.A. Berg, H. Markum and R. Pullirsch, Phys. Rev. **D59** (1999) 097504.
R.G. Edwards, U.M. Heller, J. Kiskis and R. Narayanan, Phys. Rev. Lett. **82** (1999) 4188.
- [3] E.V. Shuryak and J.J.M. Verbaarschot, Nucl. Phys. **A560** (1993) 306.
- [4] J.J.M. Verbaarschot and I. Zahed, Phys. Rev. Lett. **70** (1993) 3852.
J.J.M. Verbaarschot, Phys. Lett. **B329** (1994) 351; Phys. Rev. Lett. **72** (1994) 2531; Nucl. Phys. **B426** (1994) 559.
- [5] G. Akemann, P.H. Damgaard, U. Magnea and S. Nishigaki, Nucl. Phys. **B487** (1997) 721.
P.H. Damgaard and S.M. Nishigaki, Nucl. Phys. **B518** (1998) 495.
M.K. Şener and J.J.M. Verbaarschot, Phys. Rev. Lett. **81** (1998) 248.
T. Nagao and S.M. Nishigaki, hep-th/0001137, hep-th/0003009.
G. Akemann and E. Kanzieper, hep-th/0001188.
- [6] M.E. Berbenni-Bitsch, S. Meyer, A. Schäfer, J.J.M. Verbaarschot and T. Wettig, Phys. Rev. Lett. **80** (1998) 1146.
M.E. Berbenni-Bitsch, S. Meyer, T. Wettig, Phys. Rev. **D58** (1998) 071502.
P.H. Damgaard, U.M. Heller and A. Krasnitz, Phys. Lett. **B445** (1999) 366.
M. Göckeler, H. Hehl, P.E.L. Rakow, A. Schäfer and T. Wettig, Phys. Rev. **D59** (1999) 094503.
R.G. Edwards, U.M. Heller and R. Narayanan, Phys. Rev. **D60** (1999) 077502.
F. Farchioni, I. Hip, C.B. Lang and M. Wohlgenannt, Nucl. Phys. **B549** (1999) 364.
- [7] P.H. Damgaard, Phys. Lett. **B424** (1998) 322.
G. Akemann and P.H. Damgaard, Nucl. Phys. **B519** (1998) 682; Phys. Lett. **B432** (1998) 390.
S.M. Nishigaki, P.H. Damgaard and T. Wettig, Phys. Rev. **D58** (1998) 087704.
- [8] J.C. Osborn, D. Toublan and J.J.M. Verbaarschot, Nucl. Phys. **B540** (1998) 317.
P.H. Damgaard, J.C. Osborn, D. Toublan and J.J.M. Verbaarschot, Nucl. Phys. **B547** (1999) 305.
D. Toublan and J.J.M. Verbaarschot, Nucl. Phys. **B560** (1999) 259.
- [9] P.H. Damgaard and K. Splittorff, hep-th/9912146; hep-lat/0003017.
P.H. Damgaard, hep-lat/0001002.

- [10] H. Leutwyler and A. Smilga, Phys. Rev. **D46** (1992) 5607.
- [11] E.T. Tomboulis and L.G. Yaffe, Phys. Rev. Lett. **52** (1984) 2115.
- [12] R. Janik, M.A. Nowak and I. Zahed, Phys. Lett. **B392** (1997) 155; Phys. Lett. **B446** (1999) 9.
- [13] G. Akemann, P.H. Damgaard, U. Magnea and S. Nishigaki, Nucl. Phys. **B519** (1998) 682.
- [14] A.D. Jackson and J.J.M. Verbaarschot, Phys. Rev. **D53** (1996) 7223.
A.D. Jackson, M.K. Şener and J.J.M. Verbaarschot, Nucl. Phys. **B479** (1996) 707.
T. Guhr and T. Wettig, Nucl. Phys. **B506** (1997) 589.
- [15] M.J. Bowick and E. Brézin, Phys. Lett. **B268** (1991) 21.
E. Kanzieper and V. Freilikher, Phys. Rev. **E55** (1997) 3712.
- [16] P.J. Forrester, Nucl. Phys. **B402** (1993) 709.
- [17] J.B. Kogut, J.-F. Lagaë and D.K. Sinclair, Phys. Rev. **D58** (1998) 054504.
- [18] J. Smit and J.C. Vink, Nucl. Phys. **B286** (1987) 485.
- [19] P.H. Damgaard, U.M. Heller, R. Niclasen and R. Rummukainen, Phys. Rev. **D61** (2000) 014501.
- [20] F. Farchioni, I. Hip and C.B. Lang, Phys. Lett. **B471** (1999) 58.
- [21] F. Farchioni, Ph. de Forcrand, I. Hip, C.B. Lang and K. Splittorff, hep-lat/9912004.
- [22] R.G. Edwards, U.M. Heller, J. Kiskis and R. Narayanan, hep-lat/9910041.
- [23] J. Fingberg, U.M. Heller and F. Karsch, Nucl. Phys. B **392**, 493 (1993).
- [24] B. Bunk, K. Jansen, M. Lüscher, H. Simma, DESY report Sept. 1994.
T. Kalkreuter and H. Simma, Comp. Phys. Comm. **93** (1996) 33.
- [25] F.R. Brown *et al.*, Phys. Lett. **B251** (1990) 181.
- [26] C. Bernard *et al.*, Phys. Rev. Lett. **98** (1997) 253.
- [27] S. Chandrasekharan *et al.*, Phys. Rev. Lett. **82** (1999) 2463.